

# First-order Mott transition and its critical endpoint in a quasi-two-dimensional organic conductor, $\kappa$ -(BEDT-TTF)<sub>2</sub>Cu[N(CN)<sub>2</sub>]Cl

F. Kagawa,<sup>1</sup> T. Itou,<sup>1</sup> K. Miyagawa,<sup>1</sup> and K. Kanoda<sup>1,2</sup>

<sup>1</sup>*Department of Applied Physics, University of Tokyo,*

*Bunkyo-ku, Tokyo 113-8656, Japan*

<sup>2</sup>*CREST, Japan Science and Technology Corporation (JST)*

(Dated: February 7, 2020)

An organic Mott insulator,  $\kappa$ -(BEDT-TTF)<sub>2</sub>Cu[N(CN)<sub>2</sub>]Cl, was investigated by resistance measurements under hydrostatic He gas pressure at zero and high magnetic fields. The resistance variation against pressure shows clear jump and hysteresis below 38 K, while it is continuous at the higher temperatures. This means that the first-order Mott transition has a critical endpoint at 38 K, where it changes into the crossover, analogous to the liquid-gas transition. The endpoint is characterized by critical divergence in pressure derivative of resistance,  $|\frac{1}{R} \frac{\partial R}{\partial P}|$ , vanishing of the resistance jump, and closing of the effective charge gap. The pressure-temperature phase diagrams under a zero field and a high magnetic field are presented.

The Mott transition is one of the metal-insulator transitions (MIT) which are representative phenomena in highly correlated electrons. The family of quasi-two-dimensional organic conductors,  $\kappa$ -(BEDT-TTF)<sub>2</sub>X, are model systems for the study of the Mott transition in two dimensions, where BEDT-TTF is bis(ethylenedithio)tetrathiafulvalene and X stands for various kinds of anions. They have layered structures with the conducting BEDT-TTF layers and the insulating anion layers. In the conducting layer, the BEDT-TTF dimers form anisotropic triangular lattice, and the dimer band is half-filled [1]. The salt of X = Cu[N(CN)<sub>2</sub>]Cl (denoted as  $\kappa$ -Cl hereafter) is an antiferromagnetic insulator (AFI) with a commensurate order at ambient pressure and thus is understood as a Mott insulator driven by the strong electron correlation [2]. When  $\kappa$ -Cl is pressurized, it becomes metallic and undergoes a superconducting transition at  $T_C \sim 13$  K under a pressure of 0.3 kbar [3]. It is considered that the pressure induces the Mott transition. On the other hand, the salts of X = Cu[N(CN)<sub>2</sub>]Br and X = Cu(NCS)<sub>2</sub> behave like the pressurized  $\kappa$ -Cl with superconducting ground states [4]. The metallic states are found to have strong electron correlation by the <sup>13</sup>C-NMR study [5]. Thus, the pressure and the replacement of anion X, which is equivalent to discrete pressure control [1], are quite effective to drive the Mott transition in the organics. Moreover, since they have no orbital degree of freedom, they give a prototype of the Mott transition. These aspects make the organics suitable for pursuing the fundamentals of the Mott transition both experimentally [1] and theoretically [6, 7].

The critical behavior near MIT is a key to the comprehension of the Mott transition. However, the criticality of the Mott transition still remains open, because most of the previous experiments have been performed under the chemical or discrete hydrostatic pressure control [3, 5, 8]. In this respect,  $\kappa$ -Cl situated in the vicinity of the Mott transition is advantageous because it can

enter into the critical regime of the Mott transition by soft pressure, which can be controlled with high accuracy. Recent ac susceptibility and NMR study [9] and ultrasonic study [10] under continuously variable He gas pressure have revealed the pressure-temperature (P-T) phase diagram and the charge compressibility characteristics of  $\kappa$ -Cl. In the present work, we have performed resistance measurements for  $\kappa$ -Cl under the He gas pressure at a zero field and 11 T above the upper critical field,  $H_{C2}$ . Here, we report huge resistance jump, which unambiguously evidences the first-order Mott transition, and critical behaviors of the transition endpoint, which is analogous to the liquid-gas transition. The zero-field and high-field P-T phase diagrams are also presented.

The size of the  $\kappa$ -Cl crystal used here is  $1.8 \times 1.4 \times 1.2$  mm<sup>3</sup>. The in-plane resistance was measured with the standard dc four-probe method. The sample was mounted in the Be-Cu cell and pressurized by compressing the He gas. To obtain the resistive diagram in the pressure-temperature plane, the measurements were performed under both isothermal pressure sweep and isobaric temperature sweep. In the isothermal process, the pressure sweep was made so slowly that the temperature deviation was within  $\pm 50$  mK. During the isobaric temperature sweep, which requires more care because the temperature sweep inevitably causes pressure change, the He gas inflow (outflow) to (from) the cell was finely controlled so that the pressure derivation was maintained within  $\pm 0.05$  MPa. To ensure the hydrostatic nature of pressure, the present experiments were performed except the P-T region of the He solidification. In order to avoid the possible affect of the conformational disorder in the ethylene groups of BEDT-TTF, the sample was cooled sufficiently slowly (0.1 K/min) around 70 ~ 100 K where the vibration of the ethylene groups is considered to be frozen [8]. As for the experiments under a high field, we applied 11 T, which is much higher than the  $H_{C2}$  in the temperature range studied here, normal to the conduct-

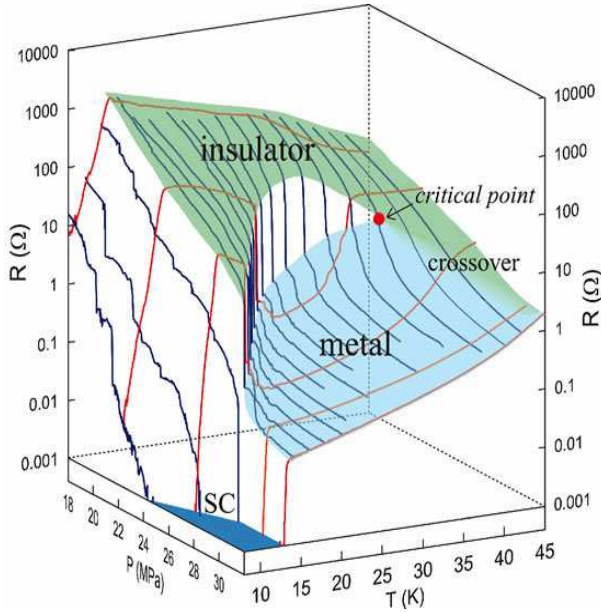


FIG. 1: Overview of resistance behavior around the Mott transition against pressure and temperature in  $\kappa$ -Cl. Blue and red lines are the data taken under isothermal pressure sweep and isobaric temperature sweep, respectively.

ing layer.

The overall feature of the present results around the Mott transition is visualized in a pressure ( $P$ ) - temperature ( $T$ ) - resistance ( $R$ ) diagram shown in Fig. 1, where blue and red curves are data taken under the isothermal pressure sweep and the isobaric temperature sweep, respectively. At low pressures, the system is highly resistive with non-metallic temperature dependence ( $\partial R / \partial T < 0$ ), while at high pressures it is conductive with metallic temperature dependence ( $\partial R / \partial T > 0$ ). The transition between the two regimes occurs with a huge resistance jump on a well-defined line in the P-T plane. It is also seen that the resistive jump becomes diminished at elevated temperatures and eventually vanishes at a certain critical point, above which the resistance variation is continuous. At low temperatures below 13 K, superconductivity appears at a high pressure region and even in the low pressure side the resistance decrease with temperature is observed. The data of the pressure dependence are classified into three temperature regions of  $T > 38$  K,  $38$  K  $> T > 13$  K ( $\sim T_C$ ), and  $T < 13$  K, which are discussed in detail below.

As an example of the behaviors at higher temperatures above 38 K, the data at 40.1 K are shown in Fig. 2 (a), where neither anomaly nor hysteresis is observed. Since the temperature derivative of resistance,  $\partial R / \partial T$ , is changed from negative to positive by pressure (see Fig. 1), the resistance variation against pressure is regarded as crossover from insulator to metal. As seen in Fig. 2 (b), the variation gets steeper with temperature de-

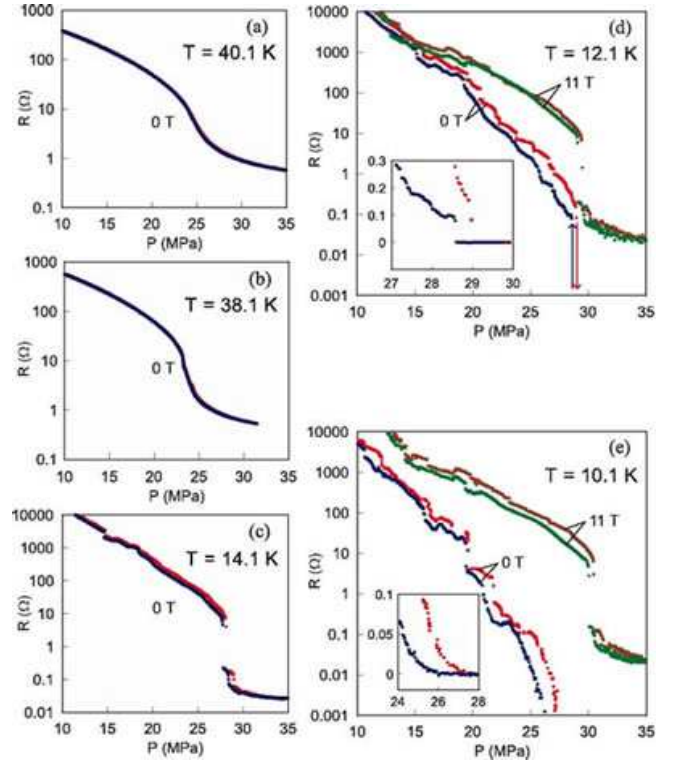


FIG. 2: Isothermal pressure dependence of resistance at various temperatures. The red and blue points are the data taken under ascending and descending pressures, respectively, at a zero field ((a) - (e)), while the brown and green points are under ascending and descending pressures at a field of 11 T ((d) and (e)). Insets of (d) and (e) are enlarged views of each main panel in linear scales around the pressure where the resistance vanishes under a zero field.

creased. One can define a crossover pressure at which the pressure derivative of resistance,  $|\frac{1}{R} \frac{\partial R}{\partial P}|$ , shows a peak as shown in Fig. 3. The peak grows as temperature approaches 38.1 K, where it is divergent (see the inset of Fig. 3). Namely, the  $|\frac{1}{R} \frac{\partial R}{\partial P}|$  is divergent around the critical point of  $(P_C, T_C) = (23.2 \text{ MPa}, 38.1 \text{ K})$  roughly as  $\sim (P_C - P)^{-0.55 \pm 0.1}$  against pressure in a range of  $P_C - P \leq 3 \text{ MPa}$  and as  $\sim (T - T_C)^{-0.9 \pm 0.1}$  against temperature along the crossover. The criticality should be related to divergence in the charge compressibility observed experimentally [10] and predicted theoretically [11, 12].

Below 38 K, the resistive crossover is changed into the resistive transition of the first-order, which is evidenced by the resistance jump and hysteresis. Shown in Fig. 2 (c) are the data at 14.1 K, where the magnitude of the jump at 28.1 MPa amounts to nearly two orders of magnitude and a small hysteresis of  $\sim 0.3$  MPa larger than the experimental error of  $\sim 0.1$  MPa is appreciable. This behavior is a clear evidence of the first-order Mott transition. The huge resistive jump indicates a bulky transition. Additional small jumps and slightly irreversible resistance traces extended around the bulk

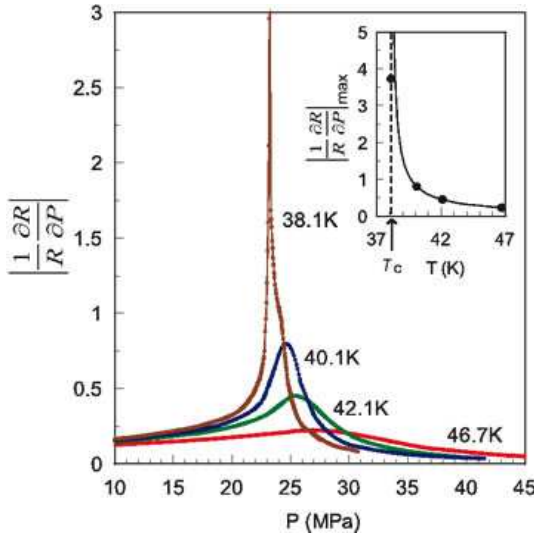


FIG. 3: The pressure derivative of resistance,  $|\frac{1}{R} \frac{\partial R}{\partial P}|$ , against pressure at several temperatures. The value of  $|\frac{1}{R} \frac{\partial R}{\partial P}|_{\max}$  is plotted against temperature in the inset. The arrow indicates the critical temperature, 38.1 K, determined by disappearance of the resistance jump. The divergence is described by the solid curve of  $\sim (T - T_C)^{-0.9}$  when  $T_C$  is fixed at 38.1 K.

transition are likely to come from inhomogeneous internal pressure in the sample, although the possibility of intrinsic phase separation with only tiny fraction of the secondary phase is not ruled out. As temperature is increased, the magnitude of the resistive jump decreases with the hysteresis diminished and eventually vanishes at the critical point, (23.2 MPa, 38.1 K) [13], where the first-order MIT changes to the crossover. The resistive behavior under a field of 11 T was indistinguishable from the zero-field case above 13 K in the pressure scale of Fig. 2 (not shown), meaning no significant field-dependence of the MIT.

At lower temperatures below 13 K, where superconductivity appears under pressure at a zero field, the effect of the magnetic field is prominent. The data at 12.1 K under a zero field and 11 T are shown in Fig. 2 (d). At a zero field, the resistance suddenly vanishes around 29.0 MPa with large hysteresis against pressure, indicating the bulky SC-insulator transition (SIT) of the first-order. By application of 11 T, the SIT was converted into MIT with the transition pressure nearly unchanged. It is seen that the field dependence of resistance is large even in the low pressure region below 28.5 MPa. It is considered that tiny SC domains are induced progressively in the insulating host phase by pressure at a zero field but are destroyed at 11 T [14]. At 10.1 K (Fig. 2 (e)), the resistance under a zero field decreases continuously and falls below the noise level around  $\sim 27$  MPa, where the growing SC fraction is considered to be percolated before occurrence of the bulky SIT at a higher pressure. Actually a bulky MIT under 11 T was at a higher pressure,

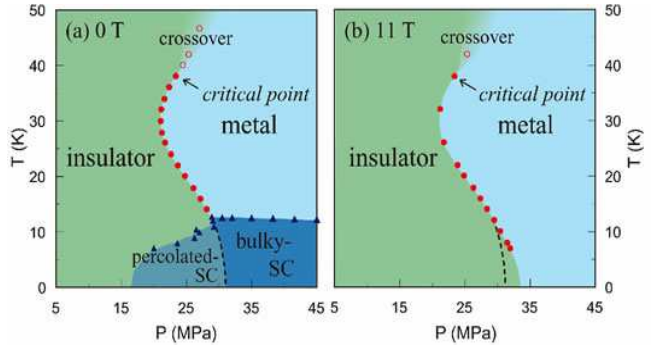


FIG. 4: Pressure-temperature phase diagrams of  $\kappa$ -Cl under a zero field (a) and a field of 11 T (b). Closed red circles and open red circles represent points at which resistance shows jump (first-order transition) and  $|\frac{1}{R} \frac{\partial R}{\partial P}|$  is maximum (crossover point), respectively. The superconducting transition defined by the resistance vanishing is marked by closed blue triangles. The same broken lines drawn in both diagrams are taken after Lefebvre *et al.* [7] and represent the bulky SIT boundary.

30.4 MPa, as seen in Fig. 2 (e). According to the previous work by NMR [9], the drastic exchange of the volume fractions of AFI and SC phases occurs at a certain pressure (broken lines shown in Fig. 4).

Figure 4 shows the P-T phase diagrams of  $\kappa$ -Cl under a zero field (a) and 11 T (b), where the closed and open red circles represent points giving the resistance jumps (first-order transition) and maximum  $|\frac{1}{R} \frac{\partial R}{\partial P}|$  (crossover), respectively, and the superconducting transition defined by the resistance vanishing is marked by closed blue triangles. Figure 4 (a) is consistent with the Lefebvre's diagram [9], after which the broken line is drawn as a bulk SIT line. Comparing the phase diagrams under zero and high fields, one finds that the MIT lines are nearly the same above 13 K while, below that, the MIT line under 11 T is located to the higher pressure side than the bulk SIT line. Since the magnetic field is expected to have no significant influence on the free energy of the metal and insulator because of the small spin susceptibility [5], it is reasonable that the MIT line above 13 K ( $\sim T_C$ ) is field-insensitive. Below 13 K, however, the free energy of the SC phase at a zero field should be lower than that of the metallic phase at zero and 11 T; namely,  $F_{SC, 0T} < F_{metal, 0T} \simeq F_{metal, 11T}$ . Therefore the more stable SC phase is extended with the SIT line pushed to the lower pressure side. As temperature increased, the free energy difference should be diminished and vanish at  $T_C$ . This also explains that the separated SIT and MIT lines merge at  $T_C$ .

The competition between the neighboring AFI and SC phases as in the  $\kappa$ -(BEDT-TTF)<sub>2</sub>X family [15] has often been discussed in terms of SO(5) theory [16, 17], which treats the AF and SC orders in a unified way of the five-dimensional superspin. The SO(5) theory tells that the

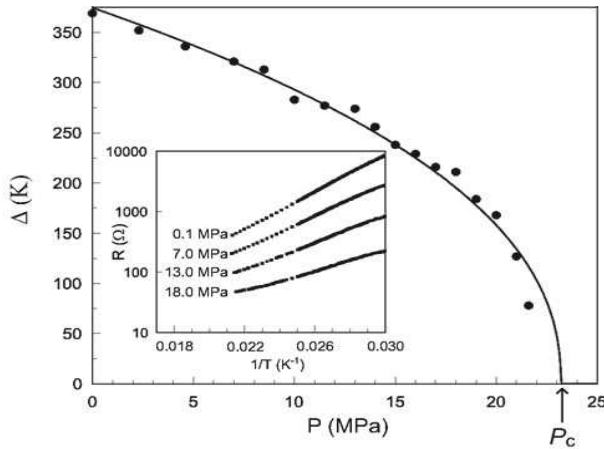


FIG. 5: Pressure-dependence of the effective charge gap. The gap,  $\Delta$ , defined by  $R \sim \exp(\Delta/T)$  is estimated from the Arrhenius plot of resistance as shown in the inset. The arrow indicates the critical pressure, 23.2 MPa, determined by disappearance of the resistance jump. The pressure dependence of the gap is described by the solid curve of  $\sim (P_C - P)^{0.4}$  when  $P_C$  is fixed at 23.2 MPa.

phase diagram has a bicritical point at the end of a first-order transition line separating the AF and SC phases in the phase diagram. The present results show that the first-order line is extended to the high temperature non-ordered region. This is beyond the scope of the SO(5) theory, which needs to be extended so as to incorporate the Mott transition [18].

We now examine the charge gap profile on the insulating side near the critical point. The inset of Fig. 5 shows the Arrhenius plot of the resistance. In a restricted temperature range from 50 K to 33 K, the data are nearly on straight lines, the slope of which gives the activation energy. The effective charge gap,  $\Delta$ , defined by  $R \sim \exp(\Delta/T)$  is shown against pressure in the main panel of Fig. 5. It is seen that the gap closes around the critical point. The overall profile of the gap closing seems to be described by a form of  $\Delta(P) \sim (P_C - P)^{0.4 \pm 0.1}$  with  $P_C = 23.2$  MPa. This is an additional criticality of the critical point.

In the course of the present work, Limelette *et al.* have reported resistivity measurements of  $\kappa$ -Cl under He gas pressure [19]. According to their experiments, the hysteresis was observed but resistivity jump was absent. They pointed out that the behavior comes from the co-existence of the insulating and metallic phases in a wide pressure range and discussed the results in terms of the dynamical mean field theory (DMFT). The results are in contrast with the present results, which clearly show sharp discontinuity in  $R(P, T)$  and the divergent criticality of the first-order endpoint [20]. The present results indicate that the Mott transition in  $\kappa$ -Cl shares the criticality in the liquid-gas transition, as was suggested by DMFT [21].

To conclude, we investigated the quasi-two-dimensional organic Mott insulator,  $\kappa$ -(BEDT-TTF)<sub>2</sub>Cu[N(CN)<sub>2</sub>]Cl, by resistance measurements under continuously variable hydrostatic pressure and obtained the pressure-temperature phase diagrams at zero and 11 Tesla. It was found that the Mott transition is accompanied by the gigantic resistive jump and the first-order transition line has an endpoint at  $(P_C, T_C) = (23.2 \text{ MPa}, 38.1 \text{ K})$ , where the transition is changed to the crossover. The endpoint is found to have several critical behaviors; (i) the resistance jump vanishes, (ii) the effective charge gap closes, and (iii) the pressure derivative of resistance,  $|\frac{1}{R} \frac{\partial R}{\partial P}|$ , is divergent, reflecting the divergence in the charge compressibility. These results show phenomenological correspondence between the Mott transition of correlated electrons and the liquid-gas transition of molecules or atoms. The field dependence of the phase diagram is explained by the free energy consideration.

The authors acknowledge N. Nagaosa, S. Onoda, and M. Imada for fruitful discussion.

---

- [1] K. Kanoda, Physica C **282-287**, 299 (1997); K. Kanoda, Hyperfine Interact. **104**, 235 (1997).
- [2] K. Miyagawa *et al.*, Phys. Rev. Lett. **75**, 1174 (1995).
- [3] J. Williams *et al.*, Inorg. Chem. **29**, 3272 (1990); Yu. V. Sushko and K. Andres, Phys. Rev. B **47**, 330 (1993); H. Ito *et al.*, J. Phys. Soc. Jpn. **65**, 2987 (1996).
- [4] H. Urayama *et al.*, Chem. Lett. **1988**, 55 (1988); A. M. Kini *et al.*, Inorg. Chem. **29**, 2555 (1990).
- [5] A. Kawamoto *et al.*, Phys. Rev. Lett. **74**, 3455 (1995); Phys. Rev. B **52**, 15522 (1995).
- [6] H. Kino and H. Fukuyama, J. Phys. Soc. Jpn. **65**, 2158 (1996).
- [7] R. H. McKenzie, Science **278**, 820 (1997); Comments Cond. Matt. Phys. **18**, 309 (1998).
- [8] H. Taniguchi *et al.*, Phys. Rev. B **67**, 014510 (2003).
- [9] S. Lefebvre *et al.*, Phys. Rev. Lett. **85**, 5420 (2000).
- [10] D. Fournier *et al.*, Phys. Rev. Lett. **90**, 127002 (2003).
- [11] G. Kotliar *et al.*, Phys. Rev. Lett. **89**, 046401 (2002).
- [12] S. Onoda and M. Imada, Phys. Rev. B **67**, 161102 (2003).
- [13] Even at 38.1 K, a small kink, which is the remnant of the jump, is appreciable. The actual critical temperature may be slightly higher than 38.1 K.
- [14] The resistance decrease with temperature below 13 K at a zero field was changed into non-metallic temperature dependence by application of 11 T.
- [15] K. Miyagawa *et al.*, Phys. Rev. Lett. **89**, 017003 (2002).
- [16] S. -C. Zhang, Science **275**, 1089 (1997).
- [17] S. Murakami and N. Nagaosa, J. Phys. Soc. Jpn. **69**, 2395 (2000).
- [18] S. Onoda and N. Nagaosa, cond-mat 0306437.
- [19] P. Limelette *et al.*, Phys. Rev. Lett. **91**, 016401 (2003).
- [20] We suppose that the discrepancy is attributable to the matter of the sample quality.
- [21] G. Kotliar *et al.*, Phys. Rev. Lett. **84**, 5180 (2000).